Measurement of strange particle femtoscopic correlations at the CMS experiment

Raghunath Pradhan for the CMS Collaboration[1,*]

[1]University of Illinois, Chicago, USA, 60607

Abstract. The two particle correlations as a function of relative momenta of identified hadrons involving K^0_S and $\Lambda/\overline{\Lambda}$ are measured in PbPb collisions at $\sqrt{s_{NN}}$ = 5.02 TeV with the data samples collected by the CMS experiment at the LHC. Such correlations are sensitive to the quantum statistics and possible final state interactions between the particles. The source radii are extracted from $K^0_S K^0_S$ correlations in different centrality regions and found to decrease from central to peripheral collisions. The strong interaction scattering parameters are extracted from $\Lambda K^0_S \oplus \overline{\Lambda} K^0_S$ and $\Lambda\Lambda \oplus \overline{\Lambda\Lambda}$ correlations using the Lednicky-Lyuboshits model, and compared with other experimental and theoretical results.

1 Introduction

Two-particle correlations in relative momentum, so-called femtoscopic correlations, arising from relativistic heavy ion collisions provide a powerful tool for studying the spatiotemporal characteristics of the particle emitting sources created in these collisions and the subsequent interactions of the emitted particles [1]. The identical particle correlations are sensitive to quantum statistics (QS) and to possible final-state interactions (FSI), while nonidentical particle correlations are only sensitive to final-state interactions. The correlations among the neutral K^0_S, Λ, and $\overline{\Lambda}$ particles, collectively referred to as V^0 particles, are of particular interest. Because of their relatively large mass, femtoscopy based on K^0_S particles is less affected by resonance decays than is the case with more commonly studied pion and charged kaon pairs [2]. The results from $K^0_S K^0_S$, $\Lambda K^0_S \oplus \overline{\Lambda} K^0_S$, and $\Lambda\Lambda \oplus \overline{\Lambda\Lambda}$ correlation studies can be used to determine the strong-interaction scattering parameters, i.e., the scattering length and the effective range, that are impossible to obtain from currently achievable scattering experiments [3–7]. This information can be used to constrain hadron-hadron correlation models that are used, for example, in modeling the composition of neutron stars [8, 9].

This note presents $K^0_S K^0_S$, $\Lambda K^0_S \oplus \overline{\Lambda} K^0_S$, and $\Lambda\Lambda \oplus \overline{\Lambda\Lambda}$ femtoscopic correlations as a function of relative momentum in PbPb collisions at $\sqrt{s_{NN}}$ = 5.02 TeV, using data recorded by the CMS experiment during the 2018 LHC run. The $K^0_S K^0_S$ correlations were measured in the extended range of centrality bin (0–60%), where centrality refers to the percentage of the total inelastic hadronic nucleus-nucleus cross section, and 0% corresponds to a maximum overlap of the colliding nuclei. The $\Lambda K^0_S \oplus \overline{\Lambda} K^0_S$ and $\Lambda\Lambda \oplus \overline{\Lambda\Lambda}$ correlations were measured in the centrality range of 0–80%. This is the first measurement of the $\Lambda\Lambda \oplus \overline{\Lambda\Lambda}$ femtoscopic correlation in

*e-mail: raghunath.pradhan@cern.ch

PbPb collisions at the LHC. The source size and strong interaction parameters are determined using the Lednický–Lyuboshitz (LL) model [11] and compared with theoretical calculations and results from other experiments.

2 $K^0_S K^0_S$, $\Lambda K^0_S \oplus \overline{\Lambda} K^0_S$, and $\Lambda\Lambda \oplus \overline{\Lambda\Lambda}$ femtoscopic correlations

The $K^0_S K^0_S$ correlations as a function of relative momenta of the particle pair $q_{\rm inv}$ [1, 12], shown in Fig. 1, measured in the six centrality bins with $0 < k_{\rm T} < 2$ GeV, where $k_{\rm T} \equiv |\vec{p}_{\rm T,1} + \vec{p}_{\rm T,2}|/2$ is the average transverse momentum of the particle pair [12]. The size of the particle-emitting source $R_{\rm inv}$ extracted from $K^0_S K^0_S$ correlation using the LL fit [11] together with nonfemtoscopic background [12] for different centrality ranges and plotted in the left panel of figure 2. It can be seen that $R_{\rm inv}$ decreases from central (0–10%) to peripheral (50–60%) events, as expected from a simple geometric picture of the collisions. The right panel of figure 2 shows CMS and ALICE results for $R_{\rm inv}$ as a function of transverse mass $m_{\rm T}$ in three centrality bins. The transverse mass can be calculated as $m_{\rm T} = \sqrt{(m_{\rm inv}/2)^2 + k_{\rm T}^2}$, where $m_{\rm inv}$ is the invariant mass of the two-particle system [12]. Extrapolations of the $m_{\rm T}$ dependence found for the ALICE results at $\sqrt{s_{\rm NN}} = 2.76$ TeV [13] to the $m_{\rm T}$ values of the CMS results at $\sqrt{s_{\rm NN}} = 5.02$ TeV shows consistent results for the two experiments.

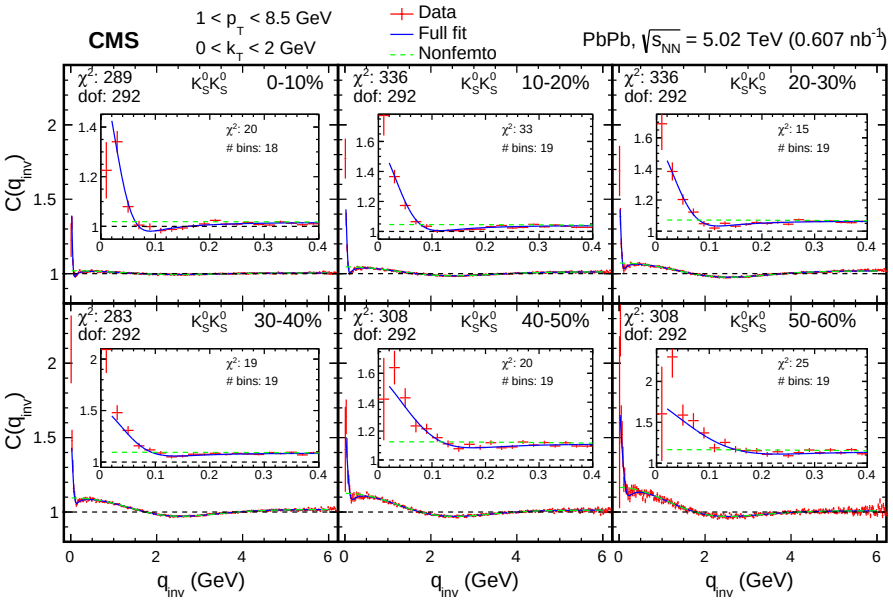

Figure 1. The correlation distributions and fits for $K^0_S K^0_S$ pairs in different centrality ranges, starting from 0–10% centrality to 50–60% centrality, with $0 < k_{\rm T} < 2$ GeV. In each plot, the red circles represent the data, the blue solid line is the fit, and the green dashed line is the nonfemtoscopic background. The χ^2 and dof values are for the full $q_{\rm inv}$ range. The insert plots show the data and the fit for the $q_{\rm inv} < 0.4$ GeV region, with the χ^2 and number of bins evaluated in that region.

Figure 3 shows the $\Lambda K^0_S \oplus \overline{\Lambda} K^0_S$ (left) and $\Lambda\Lambda \oplus \overline{\Lambda\Lambda}$ (right) correlation measurements in 0–80% centrality with no restriction on $k_{\rm T}$ [12]. The strong interaction scattering parameters: real scattering length ($\Re f_0$), imaginary scattering length ($\Im f_0$), and effective range (d_0), were extracted from the $\Lambda K^0_S \oplus \overline{\Lambda} K^0_S$ and $\Lambda\Lambda \oplus \overline{\Lambda\Lambda}$ correlations using LL fit [11] together with nonfemtoscopic background [12]. Figure 4 shows d_0 versus $\Re f_0$ (left) and $\Im f_0$ versus $\Re f_0$

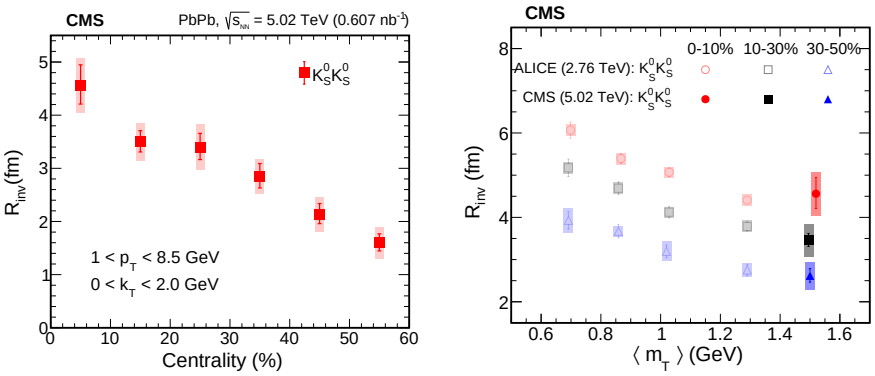

Figure 2. Left: The R_{inv} (left) as a function of centrality. Right: The R_{inv} (left) as a function of $\langle m_{\mathrm{T}} \rangle$ for the three centrality bins (0–10%, 10–30%, and 30–50%) from this analysis (dark filled symbols) and from the ALICE experiment (light open symbols) [13]. For each data point, the lines and the shaded areas indicate the statistical and systematic uncertainties, respectively.

(right). Comparisons to theoretical calculations and results from other experiments are also shown [12]. The negative value of $\Re f_0$ in $\Lambda\mathrm{K}^0_\mathrm{S} \oplus \overline{\Lambda}\mathrm{K}^0_\mathrm{S}$ correlations suggests that the $\Lambda\mathrm{K}^0_\mathrm{S}$ ($\overline{\Lambda}\mathrm{K}^0_\mathrm{S}$) interaction is repulsive while $\Im f_0$ is consistent with zero within uncertainty, precluding any definitive claims regarding possible inelastic processes [12]. A positive $\Re f_0$ value for the $\Lambda\Lambda \oplus \overline{\Lambda\Lambda}$ correlations indicates that the $\Lambda\Lambda$ ($\overline{\Lambda\Lambda}$) interaction is attractive.

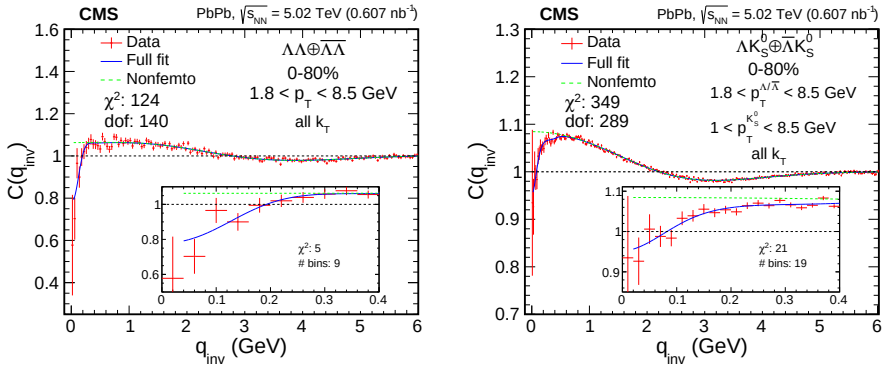

Figure 3. The correlation distributions and fits for $\Lambda\mathrm{K}^0_\mathrm{S} \oplus \overline{\Lambda}\mathrm{K}^0_\mathrm{S}$ (left) and $\Lambda\Lambda \oplus \overline{\Lambda\Lambda}$ (right) pairs with 0–80% centrality and no restriction on k_{T}. the red circles represent the data, the blue solid line is the fit, and the green dashed line is the non-fetoscopic background. The χ^2 and dof values are for the full q_{inv} range. The insert plots show the data and the fit for the $q_{\mathrm{inv}} < 0.4$ GeV region, with the χ^2 and number of bins evaluated in that region.

3 Summary

The $\mathrm{K}^0_\mathrm{S}\mathrm{K}^0_\mathrm{S}$, $\Lambda\mathrm{K}^0_\mathrm{S} \oplus \overline{\Lambda}\mathrm{K}^0_\mathrm{S}$, and $\Lambda\Lambda \oplus \overline{\Lambda\Lambda}$ femtoscopic correlations are studied using lead-lead (PbPb) collision data at a center-of-mass energy per nucleon pair of $\sqrt{s_{\mathrm{NN}}} = 5.02$ TeV, collected by the CMS Collaboration. This is the first report on $\Lambda\Lambda \oplus \overline{\Lambda\Lambda}$ correlations in PbPb collisions at the CERN LHC. The source size R_{inv} extracted from $\mathrm{K}^0_\mathrm{S}\mathrm{K}^0_\mathrm{S}$ correlations in six centrality bins covering the 0–60% range. Along with the R_{inv}, the strong interaction scattering parameters, i.e., the complex scattering length and effective range, were extracted from

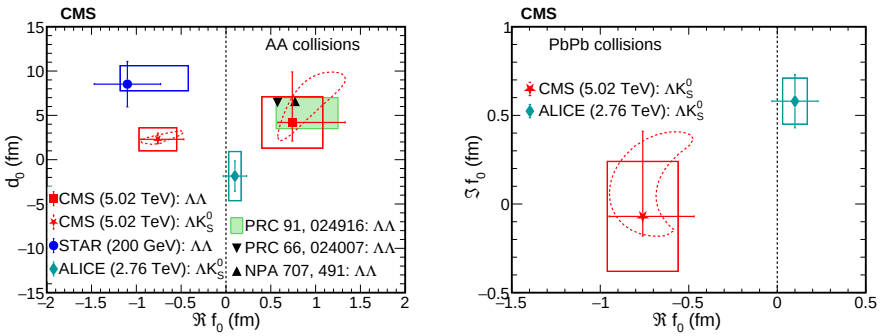

Figure 4. The measured values of d_0 versus $\Re f_0$ (left) and $\Im f_0$ versus $\Re f_0$ (right) from this analysis along with other measurements and predictions. For each data point, the lines and the boxes indicate the one-dimensional statistical and systematic uncertainties, respectively. For the CMS points, the dotted lines show two-dimensional contours corresponding to a 39% confidence level with just the statistical uncertainties included.

$\Lambda K^0_S \oplus \overline{\Lambda} K^0_S$ and $\Lambda\Lambda \oplus \overline{\Lambda\Lambda}$ correlations in the 0–80% centrality range. These scattering parameters indicate that the $\Lambda K^0_S \oplus \overline{\Lambda} K^0_S$ interaction is repulsive and that the $\Lambda\Lambda \oplus \overline{\Lambda\Lambda}$ interaction is attractive.

References

[1] M. A. Lisa, S. Pratt, R. Soltz, and U. Wiedeman, Ann. Rev. Nucl. Part. Sci. **55**, 357 (2005). https://doi.org/10.1146/annurev.nucl.55.090704.151533

[2] CMS Collaboration, Phys. Rev. C. **97**, 064912 (2018). https://doi.org/10.1103/PhysRevC.97.064912

[3] V. G. J. Stoks, R. A. M. Klomp, M. C. M. Rentmeester, and J. J. de Swart, Phys. Rev. C. **48**, 792, (1993). https://doi.org/10.1103/PhysRevC.48.792

[4] J.J de Swart and C Dullemond, Anna. Phys. **19**, 458 (1962). https://doi.org/10.1016/0003-4916(62)90185-9

[5] R. Engelmann, H. Filthuth, V. Hepp, and E. Kluge, Phys. Lett. **21**, 587 (1966). https://doi.org/10.1016/0031-9163(66)91310-2

[6] F. Eisele and H. Filthuth and W. Föhlisch and V. Hepp and G. Zech, Phys. Lett. B. **37**, 204 (1971). https://doi.org/10.1016/0370-2693(71)90053-0

[7] B. Sechi-Zorn, B. Kehoe, J. Twitty, and R. A. Burnstein, Phys. Rev. **175**, 1735 (1968). https://doi.org/10.1103/PhysRev.175.1735

[8] D. B. Kaplan and A. E. Nelson, Nucl. Phys. A. **479**, 273 (1988). https://doi.org/10.1016/0375-9474(88)90442-3

[9] Jürgen Schaffner-Bielich, Matthias Hanauske, Horst Stöcker, and Walter Greiner, Phys. Rev. Lett. **89**, 171101 (2002). https://doi.org/10.1103/PhysRevLett.89.171101

[10] CMS Collaboration, JINST **03** S08004 (2008). https://doi.org/10.1088/1748-0221/3/08/S08004

[11] R. Lednicky and V. Lyuboshits, Sov. J. Nucl. Phys. **35**, 770 (1982). https://inspirehep.net/literature/167537

[12] CMS Collaboration, CMS-PAS-HIN-21-006, https://arxiv.org/abs/2301.05290

[13] ALICE Collaboration, Phys. Rev. C. **92** 054908 (2015). https://doi.org/10.1103/PhysRevC.92.054908